



Efficacy of Aging Correction for Liquefaction Assessment of Case Histories Recorded during the 2010 Darfield and 2011 Christchurch Earthquakes in New Zealand

Salman Rahimi, S.M.ASCE¹; Clinton M. Wood, M.ASCE²; Liam M. Wotherspoon³, and Russell A. Green, M.ASCE⁴

Abstract: Data from 58 high-quality liquefaction case histories from the Darfield and Christchurch earthquakes are utilized to investigate the efficacy of current liquefaction aging correction procedures. Toward this end, liquefaction case histories are analyzed in which aging corrections are and are not applied, and the resulting predictions are compared to the actual liquefaction response of the deposits. An error-index is calculated to quantify the efficacy of aging corrections. While all the sites located in the Christchurch area are classified as Holocene, based on their geological age, their liquefaction response is influenced more by the *geotechnical* age of the soil deposits. Aging correction was determined to be beneficial for the liquefaction assessment of soils that experienced recurrent liquefaction (i.e., geotechnical young deposits). However, aging corrections were determined to exacerbate the liquefaction assessment of relatively old (greater than ~62–580 years) soil deposits. DOI: [10.1061/\(ASCE\)GT.1943-5606.0002294](https://doi.org/10.1061/(ASCE)GT.1943-5606.0002294). © 2020 American Society of Civil Engineers.

Author keywords: Soil aging; Liquefaction; Cone penetration test; Surface wave tests; Darfield earthquake; Christchurch earthquake; Geotechnical age.

Introduction

The liquefaction triggering potential of soil is commonly evaluated using the simplified stress-based procedure introduced by Whitman (1971) and Seed and Idriss (1971). This procedure involves computing two main parameters: the cyclic resistance ratio (CRR) of the soil and cyclic stress ratio (CSR) induced by the earthquake. The CRR is a measure of the soil's resistance against liquefaction triggering and can be estimated using in situ data within either a deterministic or probabilistic framework. The CSR is an estimation of the normalized shear stress induced by earthquake shaking at depth in a soil profile. To date, simplified stress-based approaches have been proposed by several researchers based primarily on the standard penetration test (SPT), the cone penetration test (CPT), and small-strain shear wave velocity (V_s) in situ test data (e.g., Andrus and Stokoe 2000; Youd et al. 2001; Cetin and Seed 2004; Moss et al. 2006; Kayen et al. 2013; Boulanger and Idriss 2014). These procedures include a large number of factors that are used to normalize/correct case histories to a moment magnitude (M_w) 7.5 earthquake (EQ), such as clean sand, 101 kPa (1 atm) vertical effective confining stress, and level ground.

However, as discussed by Seed and Idriss (1971), Youd and Hoose (1977), and Youd and Perkins (1978), Mesri et al. (1990), Arango and Migues (1996), Arango et al. (2000), Leon et al. (2006), and Hayati and Andrus (2009), the age of a soil deposit has a marked influence on the CRR or liquefaction resistance of the soil deposit, with *younger* deposits having a lower liquefaction resistance than *older* deposits. Moreover, Towhata et al. (2014) and Maurer et al. (2014) observed that deposits that experienced recurrent liquefaction were more susceptible to liquefaction in future events, on par with young deposits, regardless of the depositional age of the deposit. This implies that the occurrence of liquefaction destroys the effects of aging in soil, resulting in a geotechnically-much-younger soil deposit in terms of liquefaction resistance during future events.

Different chemical and mechanical mechanisms can be involved in soil aging. Chemical-related mechanisms are related to changes in soil cementation at particle contacts, while mechanical mechanisms involve changes in particle orientation and interlocking along with changes in soil gradation caused by particles crushing (Mitchell and Solymar 1984; Mitchell 1986; Schmertmann 1987; Mesri et al. 1990; Joshi et al. 1995; Arango and Migues 1996; Bwambale et al. 2017; Bwambale and Andrus 2019).

The effect of aging on soil has been shown to influence the penetration resistance measured from in situ tests, such as the SPT or CPT (Mitchell and Solymar 1984; Kulhawy and Mayne 1990). However, aging effects are more evident from measurements of a small-strain shear wave velocity. This is driven by the fact that the SPT blow count and CPT tip resistance are large strain measurements, which tend to be somewhat insensitive to the influence of aging, whereas V_s is a small strain measurement and thus is more sensitive to changes in the soil fabric due to aging (Andrus et al. 2007; Rahimi et al. 2018). However, neither penetration-based field testing measurements nor V_s has been shown to fully capture the aging effects of soils because of the strain level differences at which field tests are performed and age-related effects exist. Chemical-related and mechanical-related aging effects manifest in the stress-strain characteristics of soil deposit in the medium strain range

¹Graduate Research Assistant, Dept. of Civil Engineering, Univ. of Arkansas, 4190 Bell Engineering Center, Fayetteville, AR 72701.

²Associate Professor, Dept. of Civil Engineering, Univ. of Arkansas, 4190 Bell Engineering Center, Fayetteville, AR 72701 (corresponding author). ORCID: <https://orcid.org/0000-0001-5906-4154>. Email: cmwood@uark.edu

³Associate Professor, Dept. of Civil and Environmental Engineering, Univ. of Auckland, Private Bag 92019, Auckland 1142, New Zealand.

⁴Professor, Dept. of Civil and Environmental Engineering, Virginia Tech Univ., 200 Patton Hall, Blacksburg, VA 24061.

Note. This manuscript was submitted on August 14, 2019; approved on March 3, 2020; published online on May 18, 2020. Discussion period open until October 18, 2020; separate discussions must be submitted for individual papers. This paper is part of the *Journal of Geotechnical and Geoenvironmental Engineering*, © ASCE, ISSN 1090-0241.

(typically between $10^{-4}\%$ and $10^{-1}\%$), and therefore, they influence soil liquefaction resistance because the dilative and contractive behavior of soils, and thus, pore pressure generation, generally initiate in this strain range (Ishihara 1996). However, such effects will not be fully evident in large (penetration tests) or small (shear wave velocity) strain tests (Roy et al. 1996; Hayati and Andrus 2009).

In the last two decades, several studies have been conducted to develop a practical procedure to account for the aging effects of sands for liquefaction assessment purposes. Arango et al. (2000) proposed an age correction factor, which was subsequently updated by several researchers (Lewis et al. 2004; Andrus et al. 2004; Hayati et al. 2008; Hayati and Andrus 2009; Andrus et al. 2009; Maurer et al. 2014; Saftner et al. 2015). The age correction factor, K_{DR} , is typically applied to the CRR of soils

$$CRR_K = CRR \times K_{DR} \quad (1)$$

where CRR_K = age-corrected cyclic resistance ratio. Hayati and Andrus (2009) have proposed two correlations for estimating K_{DR} : one derived from cyclic triaxial and cyclic simple shear test data with the reference age of 2 days and one from field tests with the reference age of 23 years. The K_{DR} equation proposed for the field test is

$$K_{DR} = 0.13 \times \log(t) + 0.83 \quad (2)$$

where t = geotechnical age of deposit in years. This equation was developed using data from sites with geotechnical ages ranging between 0.2 and 35,000,000 years, with the majority of the sites having a geotechnical age less than approximately 200 years. The geotechnical age of the deposit is the time because the most recent critical disturbance of the soil fabric, e.g., the time since the last episode of moderate-to-severe liquefaction that resulted in the loss of the particles' mechanical interlocking or breaking of chemical cementation at particles contacts, thus resetting the aging clock of the deposit. If the soil fabric has never been disrupted, then the geotechnical age is equal to the time since the initial soil deposition (i.e., geological age). A modified K_{DR} relationship was also proposed by Maurer et al. (2014) based on the CPT and liquefaction data from the 2010 to 2011 Canterbury earthquake sequence (CES), given by Eq. (3), which slightly modifies the relationship originally proposed by Hayati and Andrus (2009)

$$K_{DR} = 0.12 \times \log(t) + 0.86 \quad (3)$$

The objective of this paper is to investigate the efficacy of the aging correction procedure proposed by Hayati and Andrus (2009) for the liquefaction assessment of soils using 58 high-quality liquefaction case histories from the CES in which aging could play a key role in the liquefaction assessment of the case histories. These case histories are ideal for this purpose because the geotechnical age of the current dataset, which varies between 0.47 and ~ 109 years, is within the range of geotechnical ages used by Hayati and Andrus (2009) to develop Eq. (2). The case history database, which includes colocated CPT and V_s data along with the postevent observations, is discussed first. Then, the geotechnical age of the soil for each of the case histories is estimated using different scenarios, including the last known critical disturbance and initial deposition. The uncorrected and age-corrected case histories are then analyzed to investigate if aging corrections could improve/exacerbate the liquefaction triggering predictions as compared to the observed response. Finally, some discussions regarding the efficacy of aging corrections for liquefaction assessment of very young and relatively old soil deposits are provided.

Soil Aging Mechanisms

The aging mechanisms that change a soil's geotechnical properties, particularly its liquefaction resistance, are not yet fully understood, but there are several potential mechanisms that are believed to be responsible for increasing the CRR of soil deposits over time. This includes changes in particle orientation, particle interlocking, cementation at particle contacts, and even changes in particle size and soil fabric due to load. The chemical and mechanical mechanisms that are involved in soil aging are shown schematically in Fig. 1. In this figure, for the initial soil conditions/fresh soil deposit (age = 0), it is assumed that the soil is cohesionless ($c_i = 0$) with a void ratio equal to e_i . The time-dependent strength gains of the soil through the aging process can be divided into three groups (Groups A, B, and C in Fig. 1), as follows:

- Group A—mechanical soil aging due to the changes in soil particle orientation and interlocking during the time t_i . In this process, the cohesion of the aged deposit remains constant while its void ratio (e_f) decreases slightly due to particle reorientation resulting from the external loading applied to the soil during the time t_i . As shown in Fig. 1, the particle dimensions are exactly the same for both fresh and aged soil elements [Fig. 1(a)], but the aged deposit may have a slightly smaller void ratio, owing to the particle reorientation. This results in increased soil stiffness, soil shear strength, and liquefaction resistance for the aged deposit (Kiyota et al. 2009; Towhata et al. 2017).
- Group B—chemical soil aging due to the changes in cementation at interparticle contacts during the time t_i . During this process, the soil particles gain some adhesion at the interparticle contacts through chemical reactions. This leads to an increase in soil cohesion while the rest of geotechnical properties including a soil void ratio, and particle interlocking and orientation remain unchanged. This process is illustrated in Fig. 1(b) in which the soil void ratio and particle interlocking and orientation are the same for both freshly and aged soil elements, but some adhesion [shown in black spots in Fig. 1(b)] developed at interparticle contacts in the aged deposit (Youd and Hoose 1977; Mitchell and Solymar 1984).
- Group C—mechanical soil aging due to the variations in soil gradation. External loading can crush some soil particles and result in a new soil skeleton and soil gradation (Joshi et al. 1995; Chuhan et al. 2002). This happens more often in near-surface soils because they can be subjected to higher changes in stress levels. Changes in the stress levels can occur due to different phenomena over thousands or millions of years. An example of this phenomena is soil compaction due to surface loading. This aging mechanism is generally rare and more valid for coarse-grained than fine-grained soils due to the higher potential for particle crushing in granular coarse-grained soils (Chuhan et al. 2002). During this process, the void ratio of the soil decreases, and the soil can reach a more stable state without any change in cohesion [Fig. 1(c)].

It should be mentioned that soil aging can also occur by any combination of the three mechanisms explained previously. This depends on the age of the soil deposit because the development rate of soil aging mechanisms is different. In the short term (from minutes to a few thousand years), mechanical mechanisms typically dominate the soil aging effects, whereas in the long term, the chemical mechanisms become more considerable (Olson et al. 2001).

Liquefaction Case History Database

The database used in this study consists of 58 high-quality CPT and V_s liquefaction case histories originally published by

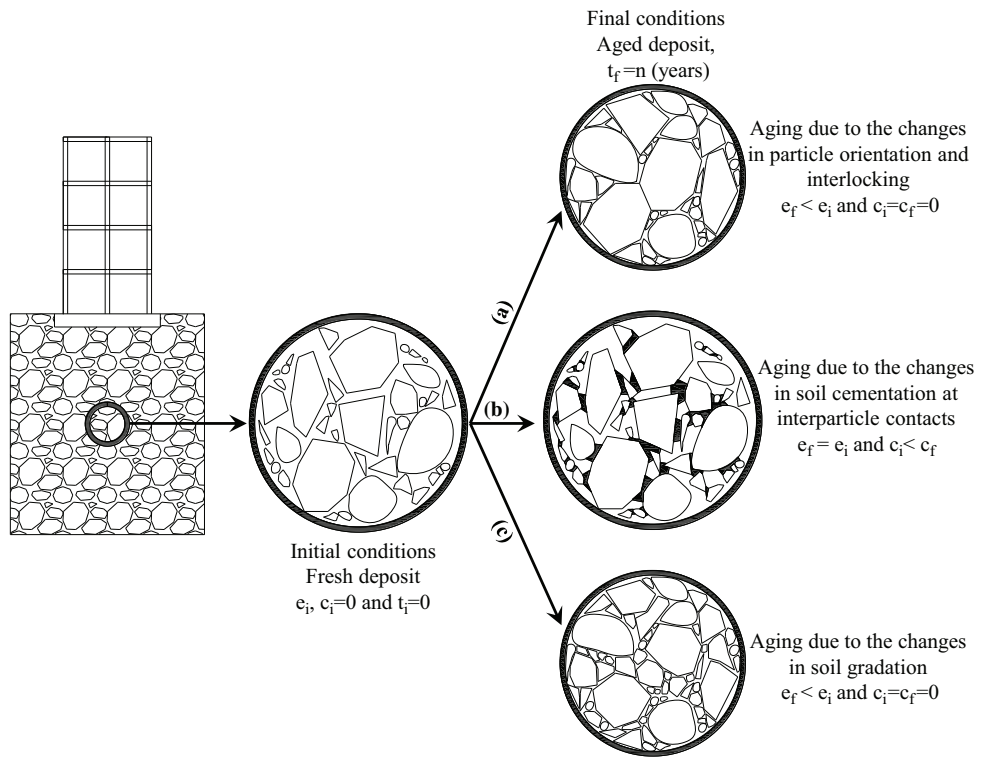


Fig. 1. Chemical and mechanical mechanisms involved in soil aging: (a) mechanical soil aging caused by changes in particle orientation and interlocking; (b) chemical soil aging caused by changes in soil cementation at particle contacts; and (c) mechanical soil aging caused by particle crushing.

Green et al. (2014), Wotherspoon et al. (2013), and Wood et al. (2017a, b). The site locations and the subsurface stratigraphy of each site are discussed in detail in these references. The case histories published by Green et al. (2014) and Wood et al. (2017a, b) consist of 44 CPT and V_s case histories (from 22 sites and 2 earthquakes), which are tabulated in Table 1, along with the location of the critical layer, the normalized/corrected CPT tip resistance (q_{c1Ncs}), and the overburden corrected, small-strain shear wave velocity (V_{s1}) for the critical layer. Surface wave methods (the spectral analysis of surface waves, multichannel analysis of surface wave, and microtremor array measurement) were used to determine the V_s of the soil profiles. This testing is discussed in detail in Wood et al. (2017a, b). The maximum lateral distance between the CPT and the center of the surface wave measurements was approximately 6 m. The severity of the surficial liquefaction manifestations for the Mw 7.1, September 4, 2010, Darfield earthquake and the Mw 6.2, February 22, 2011, Christchurch earthquake along with the approximate geotechnical and geologic age of the soils during each event are also listed in Table 1. Case histories in this study are divided into four groups in terms of liquefaction severity. These groups include the following: (1) no liquefaction, (2) minor liquefaction (limited water ejecta and cracking at the ground surface), (3) moderate liquefaction (moderate sand boils and cracking at the ground surface), and (4) severe liquefaction (considerable sand boils and cracking at the ground surface). Further details regarding these categories is provided in Green et al. (2014). The remaining 14 liquefaction case histories (from 11 sites and 1 earthquake) were published by Wotherspoon et al. (2013) and include CPT liquefaction case histories near strong motion stations (SMSs). These case histories are tabulated in Table 2 with the location of the critical layer, the q_{c1Ncs} for the critical layer, the approximate geotechnical and geologic age of the soils during the Christchurch

earthquake, the severity of the observed surficial liquefaction manifestations, and the predicted liquefaction response based on the characteristics of the recorded ground motions for the Christchurch earthquake. For liquefaction assessment using ground motion records, liquefaction was identified by observed high amplitude spikes resulting from soil dilation, followed by a reduction in the amplitude of the ground motion and a loss of high frequency content in the later part of the ground motion record (e.g., Upadhyaya et al. 2019). The CPT soundings used in the study were performed between approximately November 2010 and July 2011 following the Darfield and/or Darfield and Christchurch earthquakes. The V_s data were collected in July/August 2011 by the authors, as discussed in Wood et al. (2017a, b).

For the Green et al. (2014) and Wood et al. (2017a, b) database, there are 15 surficial manifestation and 7 no liquefaction case histories from the Darfield earthquake and 18 surficial manifestation and 4 no liquefaction case histories for the Christchurch earthquake, as presented in Table 1. For the SMSs database, there are nine liquefaction and five no liquefaction case histories based on the observed surface manifestations. However, based on the characteristics of the recorded ground motions (variations in the amplitude and high-frequency content) there are only two no liquefaction case histories in this database, as presented in Table 2. This will be subsequently explained in more detail in the paper.

Estimating Age of Soils

In the original studies by Green et al. (2014), Wotherspoon et al. (2013), and Wood et al. (2017a, b), aging corrections were not applied to the case histories. Therefore, in this study, it is necessary to estimate the age (geotechnical/geological) of each of the sites at the

Table 1. Summary of New Zealand database for the Darfield and Christchurch earthquakes

Site No.	Site name	V_{s1} (m/s)	q_{c1Ncs} (atm)	Approximate geologic age (years)	Critical layer average depth (m)	Critical layer thickness (m)	Darfield		Christchurch	
							Liquefaction incidence based on surface manifestation	Approximate geotechnical age (years)	Liquefaction incidence based on surface manifestation	Approximate geotechnical age (years)
1	SHY-09	159	71.7	3,000	4.8	2.0	No liq.	62–580	Mod liq	0.47–580
2	AVD-07	131	95.3	3,000	3.5	2.0	No liq.	62–580	Mod liq	0.47–580
3	BUR 46	129	91.6	3,000	7.3	3.0	Min liq.	62–580	Sev liq	0.47
4	CBD 21	128	147.2	3,000	5.5	2.0	No liq.	62–580	Min liq	0.47–580
5	FND 01	154	60.8	3,000	3.8	0.3	Mod liq/LatSprd	62–580	SevLatSprd ^e	0.47
6	KAN 03	132	107.9	3,000	5.2	3.0	Min liq	62–580	No liq	0.47
7	KAN 05	145	63.7	3,000	3.6	1.0	Min liq	62–580	Minor liq	0.47
8	KAN 09	153	55.1	3,000	1.9	1.2	Min liq	62–580	No liq	0.47
9	KAN 19	162	118.2	3,000	3.7	2.7	Min liq	62–580	No liq	0.47
10	KAN 23	136	127.8	3,000	4.8	1.0	Min liq	62–580	No liq	0.47
11	KAN 26	140	103.0	3,000	6.5	3.1	Mod liq	62–580	Min liq	0.47
12	KAN 28	168	71.4	3,000	2.6	1.2	Min-mod liq	62–580	Min liq	0.47
13	KAS 11	181	80.8	3,000	2.6	1.1	Min-mod liq	62–580	Min liq	0.47
14	KAS 20	137	69.3	3,000	4.3	1.5	Min-mod liq	62–580	Min liq	0.47
15	SBT 01	140	89.5	3,000	3.6	2.8	Min liq	62–580	SevLiq	0.47
16	NBT 02	142	74.4	3,000	5.8	1.9	Min-mod liq	62–580	Sev liq	0.47
17	NBT 03	108	73.7	3,000	8.6	3.2	Min liq	62–580	Sev liq	0.47
18	RCH 14	176	35.7	3,000	4.5	2.0	No liq	62–580	Min-mod liq	0.47–580
19	Z1-3	146	93.0	3,000	6.1	4.3	Min liq	62–580	Mod-sev liq	0.47
20	Z2-4	187	121.7	3,000	1.6	1.0	No liq	62–580	Mod liq	0.47–580
21	Z2-6	171	97.2	3,000	2.4	0.9	No liq	62–580	LatSprd	0.47–580
22	Z4-4	198	92.7	3,000	2.6	1.3	No liq	62–580	Mod liq	0.47–580

Note: No liq = no liquefaction; Mod liq = moderate liquefaction; Min liq = minor liquefaction; Sev liq = severe liquefaction; and SevLatSprd = severe lateral spreading.

Table 2. Summary of the SMSs database for the Christchurch earthquake

Site No.	Site name	q_{c1Ncs} (atm)	Approximate geologic age (years)	Critical layer average depth (m)	Critical layer thickness (m)	Liquefaction incidence based on surface manifestation	Liquefaction incidence based on recorded ground motions		Approximate geotechnical age (years)
							Yes	No record	
1	CCCC	87.6	3,000	2.9	0.6	Yes-minor	Yes		0.47
2	CHHC1	103.6	3,000	2.8	0.7	Yes-moderate	Yes		0.47
3	CHHC2	90.7	3,000	4.0	1.3	Yes-moderate	Yes		0.47
4	CMHS	57.8	3,000	2.3	0.6	Yes-severe	Yes		0.47
5	HPSC	54.1	3,000	2.8	2.5	Yes-severe	Yes		0.47
6	NBLC	141.1	3,000	6.1	1.0	No		No record	0.47–580
7	NNBS1	127.9	3,000	2.9	0.4	No	Yes		0.47–580
8	NNBS2	121.7	3,000	5.5	1.1	No	Yes		0.47–580
9	PPHS	70.5	3,000	3.1	0.6	No	No		0.47–580
10	PRPC1	94.3	3,000	2.7	0.3	Yes-minor	Yes		0.47
11	PRPC2	82.3	3,000	3.6	1.3	Yes-minor	Yes		0.47
12	PRPC3	102.8	3,000	2.8	0.4	Yes-minor	Yes		0.47
13	REHS	77.0	3,000	2.4	0.8	No	Yes		0.47–580
14	SHLC	103.3	3,000	3.5	0.8	Yes-moderate	Yes		0.47

time of the Darfield and Christchurch earthquakes. Because the liquefaction case histories used in this study are sites that liquefied in one or both of the earthquakes, different scenarios are considered to estimate the ages of the soil deposits, including the time since the initial deposition and the time since the last known critical disturbance. For identification of the last critical disturbance, any earthquake which was strong enough to trigger liquefaction within the soil profile can be considered as a critical disturbance, even if it did not result in surficial manifestations of liquefaction. Therefore, liquefaction manifestation may not be the best metric for estimating the geotechnical age of the soil deposits, although it is often used due to a lack of other available information. It should be mentioned

that in this study, the term *very young* soil deposits refers to soils with geotechnical ages less than the reference age (23 years) defined by Hayati and Andrus (2009), and the term *relatively old* refers to soils with geotechnical ages greater than the reference age (~62–580 years).

Darfield Earthquake

For the Darfield earthquake, two different scenarios are used to determine the geotechnical age of the soil for each case history, as follows:

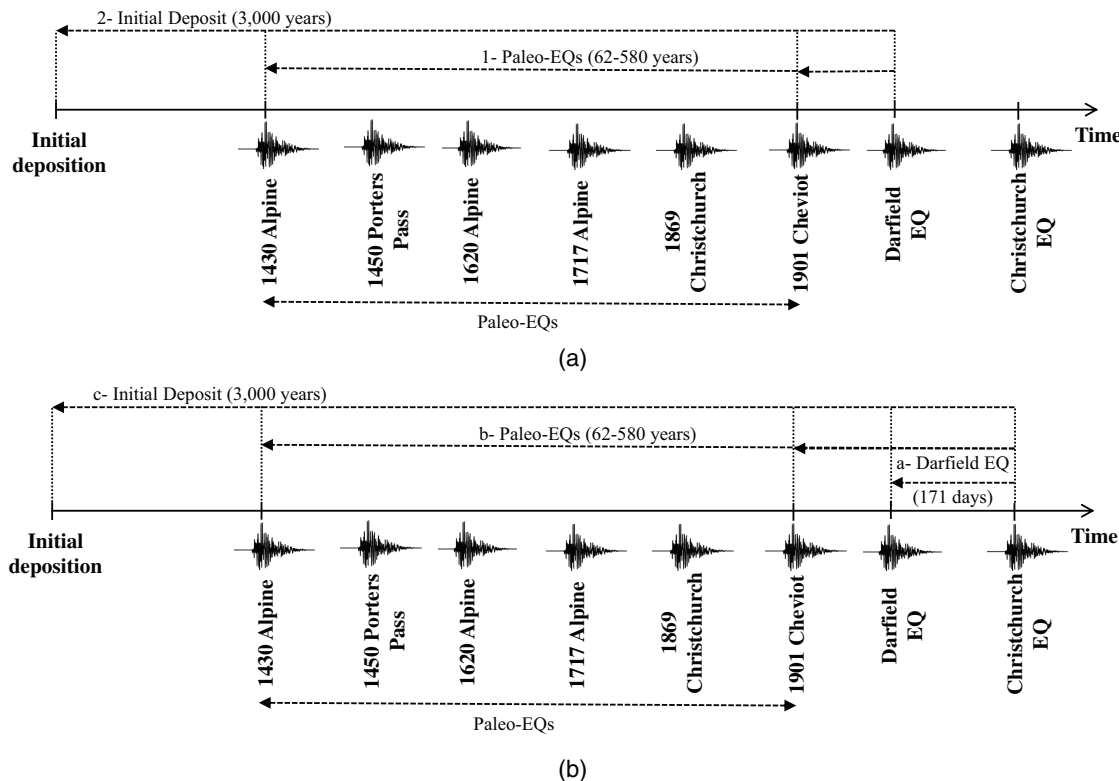


Fig. 2. Possible geotechnical and geological scenarios for age estimation: (a) Darfield case histories; and (b) Christchurch case histories.

- The age is based on the last critical disturbance [Fig. 2(a)]. Different paleo-earthquakes can be considered as the last critical disturbance for the Darfield case histories, as discussed by Bastin et al. (2016). In this study, the term *paleo-earthquakes* is defined as any prehistoric event that was not well-documented in terms of liquefaction triggering and severity. This includes seven different paleo-earthquakes that are believed to have resulted in shaking strong enough to trigger liquefaction within the soil deposits but might not have resulted in surficial manifestation, as illustrated in Fig. 2(a). Depending on the paleo-earthquake being considered as the reference point for the Darfield case histories, the geotechnical age of the soil deposits could have been between 62 and 580 years old at the time of the Darfield earthquake. Because the liquefaction response of the case history sites during these paleo-events (subsequently referred to as paleo-EQs) is unknown, it is possible that the shaking during these events was not strong enough to reset the aging clock of the soils. Therefore, another scenario that needs to be considered for the soil-age estimation at the time of the Darfield earthquake is the time since the initial deposition.
- The age is based on the initial deposition time [Fig. 2(a)]. The time since initial soil deposition (subsequently referred to as initial deposit) was determined by Cubrinovski and McCahon (2011) based on radiocarbon dating of soil samples (Cubrinovski and McCahon 2011; Brown et al. 1992). On the basis of the results of radiocarbon dating, if the initial deposit is considered as the reference point for the age estimation for the Darfield case histories, the age of the soil deposits is approximately 3,000 years at the time the Darfield earthquake occurred.

- For sites that liquefied during the Darfield earthquake, the age of the soil deposits is estimated as the number of days elapsed between the date of the Darfield and Christchurch earthquakes, i.e., 171 days [Fig. 2(b)]. This indicates that most of the sites in the Christchurch database classify as very young/fresh deposits. This scenario is referred to in this study as the Darfield earthquake.
- For sites with no observed surface manifestations of liquefaction during the Darfield earthquake (including KAN 03, KAN 09, KAN 19, and KAN 23), the age of soil deposit is estimated using three different scenarios:
 - It can be assumed that the Mw 7.1, September 4, 2010, Darfield earthquake shaking was strong enough to reset the aging clock of the deposit even though there was no evidence of liquefaction manifestation at the ground surface. This assumption is reasonable because it is supported by the results of several SMSs in which there were no surficial manifestations of liquefaction, but clear indications of liquefaction (a reduction in amplitude and high-frequency content of the ground motion records) are observed in the ground motion records. This will be subsequently explained in more detail in the paper. So, in this case, the age of deposit is the period of time between the Darfield and Christchurch earthquakes [Fig. 2(b)].
 - The age of the soil deposits can be estimated assuming liquefaction was triggering in one of the paleo-EQs but not the others [Fig. 2(b)] because no surface manifestations were observed at the ground surface at these sites following the Darfield earthquake.
 - As mentioned previously, if none of the paleo-EQs were strong enough to trigger liquefaction, the geotechnical age of soil deposits should be estimated based on the initial deposit scenario [Fig. 2(b)] (Cubrinovski and McCahon 2011; Brown et al. 1992).

Christchurch Earthquake

Sites impacted by the Mw 6.2 Christchurch earthquake can be divided into two main categorizes in terms of geotechnical age:

All the aforementioned scenarios are considered in correcting for aging effects in assessing the liquefaction potential of the case histories during the Darfield and Christchurch earthquakes.

Liquefaction Aging Correction Methodology

In the procedure proposed by Hayati and Andrus (2009) for liquefaction aging correction, the K_{DR} is applied to the CRR value. However, in this study, to be able to present all the age-corrected liquefaction case histories for each database in a single triggering plot, the reciprocal of the K_{DR} is applied to the CSR value [Eq. (4)], and the CRR curve is kept unchanged [Eq. (5)] (Fig. 3). Because the factor of safety against liquefaction, which is defined as the ratio of the CRR–CSR, will be the same regardless of whether K_{DR} is applied to CRR or $1/K_{DR}$ is applied to CSR, either of the approaches can be used for correcting for aging effects. As shown in Fig. 3, aging correction according to Hayati and Andrus (2009) can shift the cases either upward or downward depending on the geotechnical age of the soil deposits. For case histories less than 23 years old, aging correction will shift the data point upward toward the region of the predicted liquefaction triggering (Movement 1 in Fig. 3). On the other hand, for case histories with ages greater than 23 years, aging correction will shift the data point downward toward the region of no liquefaction triggering (Movement 2 in Fig. 3)

$$CSR_{\text{age-corrected}} = CSR \times (1/K_{DR}) \quad (4)$$

$$CRR_{\text{age-corrected}} = CRR_{\text{initial}} \quad (5)$$

Results and Discussion

The critical layer is defined as the layer in the profile with the lowest factor of safety against liquefaction triggering. The location of the critical layer was identified based on the CPT data (Green et al. 2014) in such a way that the depth-thickness-density combination of the critical layer for a given site is consistent with the observed liquefaction response of the site (Olson et al. 2005; Green et al. 2014, 2005). The Idriss and Boulanger (2008) CPT-based triggering procedure and the Kayen et al. (2013) V_s -based triggering procedure are used for the CPT- and V_s -based liquefaction evaluations, respectively. The Idriss and Boulanger (2008) procedure is a deterministic CPT-based approach for liquefaction assessment. The Kayen et al. (2013), V_s -based triggering procedure is presented

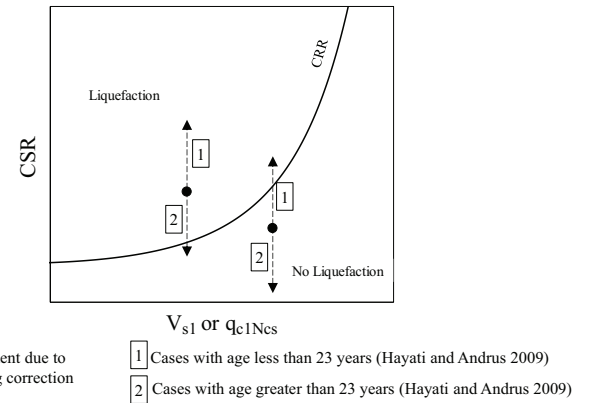


Fig. 3. Aging correction procedure used in the present study. (Reference age of 23 years is based on the Hayati and Andrus 2009 procedure.)

in a probabilistic framework; however, in this study, the deterministic triggering curve is used, which has a probability of liquefaction (P_L) = 15% per Kayen et al. (2013) for assessing the liquefaction potential of the V_s dataset. Parameters needed for liquefaction assessment of each case history are representative values of CSR, CRR, q_{c1Ncs} , and/or V_{s1} for the critical layers. These parameters were computed by averaging their values across the critical layer to develop a single value for each case history.

To investigate the influence of aging corrections on liquefaction assessments, the aging correction factors are applied to the uncorrected case histories for each database. To accomplish this goal, the liquefaction triggering plots using the uncorrected and age-corrected cases are compared with the postevent liquefaction response based on surface manifestations or recorded ground motion characteristics. An error index is used to quantify the influence of aging correction factors on the liquefaction assessment. The error index value is computed based on the error index used by Green et al. (2014) and Wood et al. (2017a, b)

$$EI = \sum_{i=1}^n Wf_i \times E_i \quad (6)$$

where n = number of case histories; Wf_i = weighting factor based on the observed liquefaction response of the deposit (Table 3); and E_i = relative error value for a given site.

The values of E_i assigned to each case history is calculated

$$E_i = \begin{cases} |CSR_{M7.5} - CRR_{M7.5}| & \text{Cases with moderate to severe evidence of liq and } CSR_{M7.5} < CRR_{M7.5} \\ 0 & \text{Cases with moderate to severe evidence of liq and } CSR_{M7.5} \geq CRR_{M7.5} \end{cases} \quad (7)$$

$$E_i = \begin{cases} |CSR_{M7.5} - CRR_{M7.5}| & \text{Cases with minor evidence of liq and } CSR_{M7.5} < CRR_{M7.5} \\ 0 & \text{Cases with minor evidence of liq and } CSR_{M7.5} \geq CRR_{M7.5} \end{cases} \quad (8)$$

$$E_i = \begin{cases} |CSR_{M7.5} - CRR_{M7.5}| & \text{Cases with no evidence of liq and } CSR_{M7.5} > CRR_{M7.5} \\ 0 & \text{Cases with no evidence of liq and } CSR_{M7.5} \leq CRR_{M7.5} \end{cases} \quad (9)$$

where $CSR_{M7.5}$ and $CRR_{M7.5}$ = cyclic stress ratio and cyclic resistance ratio for a Mw 7.5 earthquake, respectively. While the assignment of different weights based on the severity of liquefaction is somewhat subjective, the use of the weights does not influence the outcome of the study in regard to the efficacy of aging correction for liquefaction assessment.

Table 3. Weighting factors used for error index calculation

Liquefaction severity	Weighting factor (W_{f_i})
Moderate-severe	1
Minor	0.75
No liquefaction	0.5

Darfield Earthquake Case Histories

The first aging scenario used to estimate the age of soil deposits during the Darfield earthquake is the paleo-EQs. Because the actual liquefaction responses of the case history sites during the paleo-EQs are largely unknown, the Darfield case histories are first corrected for the aging effects assuming liquefaction was triggering in one of the paleo-EQs, but not the others, to find the paleo-EQ that results in the lowest error index value and number of mispredictions. Shown in Figs. 4(a and b) are the number of mispredicted case histories and error index values for the uncorrected and age-corrected CPT and V_s case histories based on the Hayati and Andrus (2009) correction procedure, using each of the paleo-EQs as the reference point for aging estimation. From Fig. 4, it can be seen that while aging corrections slightly increased the error index values for the Darfield case histories, the number of mispredicted cases significantly increased for most of the paleo-EQs scenarios. The paleo-EQs scenario that led to the lowest error index value and number of mispredictions is the 1901 Cheviot EQ; therefore, this earthquake event is considered as the last critical disturbance for aging estimation of the Darfield case histories. It should be mentioned that while it is believed that the 1901 Cheviot EQ was strong enough to trigger liquefaction within the study area (Bastin et al. 2016), it might not have resulted in severe surficial manifestation because no report is available in this regard.

In Fig. 5, the liquefaction triggering plots for the case histories from the Darfield earthquake are shown as CSR versus q_{c1Ncs} and V_{s1} . Shown in Figs. 5(a and b) are the uncorrected ($K_{DR} = 1$) case histories for CPT and V_s , respectively. The Darfield case histories are corrected for aging in Figs. 5(c and d) based on the 1901 Cheviot paleo-EQ scenario (i.e., 109 years, $K_{DR} = 1.09$), and in Figs. 5(e and f) based on the initial deposit scenario (i.e., 3,000 years, $K_{DR} = 1.28$). As may be observed from Fig. 5, the use of the aging corrections reduced the CSR for each case history, moving them toward the *no liquefaction* region as the age of the soil increases. For the case histories in which the application of

the age-correction resulted in a change in the predicted liquefaction response (e.g., predicted to liquefy without the age-correction but predicted not to liquefy after age-correction is applied), the uncorrected predicted liquefaction responses are shown by tails (vertical lines showing the aging correction) in Figs. 5(c–f).

As shown in Figs. 5(c and d), aging corrections using the 1901 Cheviot paleo-EQ scenario resulted in one additional false-negative prediction (i.e., liquefaction not predicted, but liquefaction manifestations were observed) for the CPT case histories and one additional false-negative prediction for the V_s case histories [as illustrated in Figs. 5(c and d)], resulting in a net increase of two for the number of mispredicted case histories. For the initial deposit scenario, aging corrections resulted in one additional true-negative and six additional false-negative predictions [as illustrated in Figs. 5(e and f)], resulting in a net increase of five mispredicted case histories. A summary of the error index values and number of mispredictions for each scenario is shown in Fig. 6. It should be mentioned that there are two true-positive case histories for the 1901 Cheviot paleo-EQ scenario [two CPT case histories in Fig. 5(c)] and three true-positive case histories for the initial deposit scenario (two CPT case histories and one V_s case history) that are located slightly above the CRR curve, close to the no liquefaction region. While these case histories are considered as being correctly predicted in this study ($FS < 1.0$), they are likely within the level of uncertainty of the simplified liquefaction procedure [i.e., the factor of safety (FS) of these case histories is only slightly below 1.0, meaning that the probability of liquefaction is 16%–20%, which is well below the median $P_L = 50\%$].

Overall, correcting for aging effects for the Darfield case histories using the Cheviot paleo-EQ and initial deposit scenarios exacerbated the liquefaction assessment of the Darfield case histories by increasing the number of mispredicted case histories, as shown in Fig. 6. Some minor or moderate-to-severe liquefaction cases that are correctly predicted when no-aging corrections are applied move to the no-liquefaction region when aging corrections are applied. Examining the age-corrected cases associated with the two reference ages of Cheviot paleo-EQ and the initial deposit in Figs. 5 and 6, it is observed that the initial deposit scenario resulted in a higher error index and number of mispredicted case histories in comparison with that of the Cheviot paleo-EQ scenario. If it is assumed that the aging correction relationship is accurate, which implies that the initial deposition time is unlikely to be the true reference point for the age-estimation of the Darfield case histories.

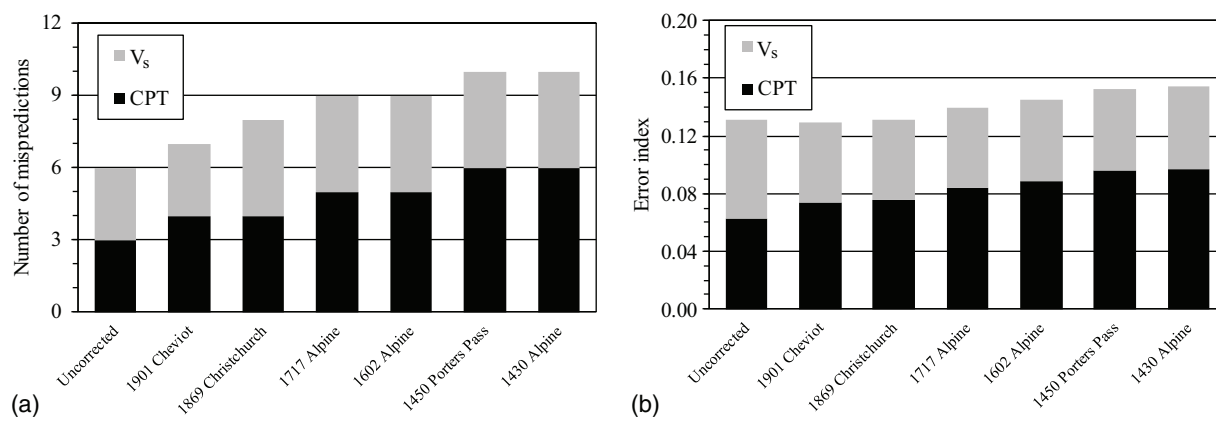


Fig. 4. Evaluation of aging correction efficacy for liquefaction assessment of the Darfield earthquake using V_s and CPT case histories and all the paleo-EQs as the reference point: (a) number of mispredicted case histories; and (b) error index.

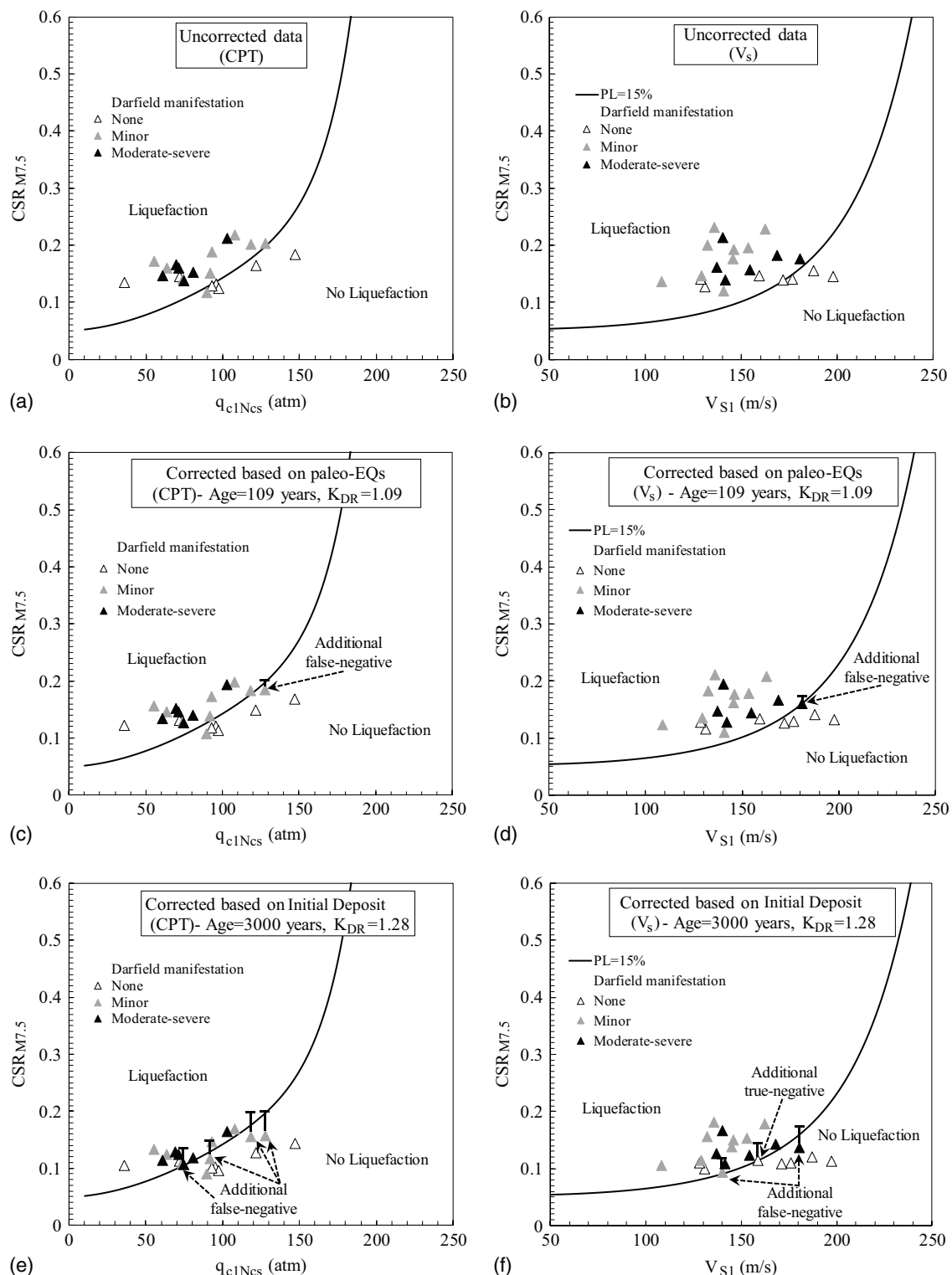


Fig. 5. Uncorrected and age-corrected CPT and V_s liquefaction case histories for the Darfield earthquake analyzed using the Idriss and Boulanger (2008) and Kayen et al. (2013) triggering procedures: (a) uncorrected data for CPT; (b) uncorrected data for V_s ; (c) age-corrected data for CPT based on the 1901 Cheviot paleo-EQ; (d) age-corrected data for V_s based on the 1901 Cheviot paleo-EQ; (e) age-corrected data for CPT based on the initial deposit; and (f) age-corrected data for V_s based on the initial deposit.

Christchurch Earthquake Case Histories

The uncorrected and age-corrected liquefaction case histories for the Christchurch earthquake are presented in Fig. 7. Plotted in Figs. 7(a and b) are the uncorrected cases for the Christchurch case

histories resulting from the CPT and V_s testing, respectively. Initially, three scenarios were going to be used to estimate the geotechnical age of soils for the Christchurch earthquake (Fig. 2). However, because the initial deposit scenario for the Darfield database led to the highest error index values and number of

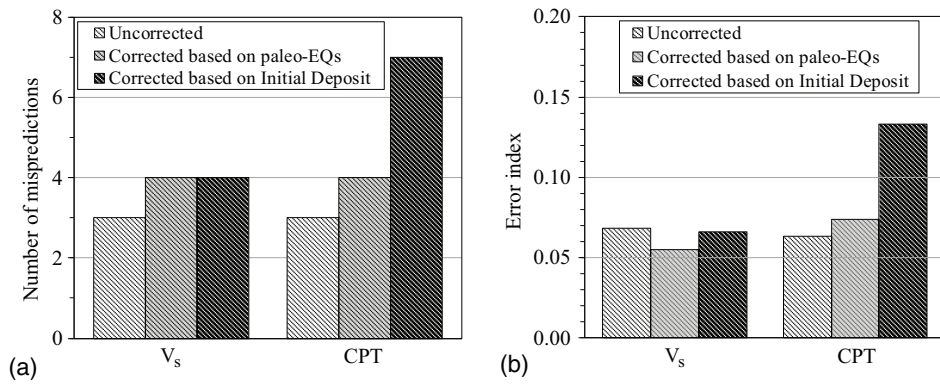


Fig. 6. Evaluation of aging correction efficacy for liquefaction assessment of the Darfield earthquake using V_s and CPT case histories: (a) number of mispredicted case histories; and (b) error index.

mispredictions (Fig. 6), only the Darfield EQ and the 1901 Cheviot paleo-EQ scenarios are considered as the reference points to estimate the age of soils for the Christchurch earthquake case histories. Therefore, the Christchurch case histories are corrected for aging effects using these two scenarios in Figs. 7(c–f). The aging corrections applied in Figs. 7(c and d) were estimated based on the Darfield EQ scenario (age = 171 days and $K_{DR} = 0.79$) for all of the case histories regardless of whether surface manifestations were or were not observed at these sites. In Figs. 7(e and f), the ages of the soil deposits were estimated based on the observed surficial liquefaction manifestations at the respective case history sites following the Darfield earthquake. For sites with surficial liquefaction manifestations, the age of the soil is set at 171 days based on the Darfield EQ scenario. For sites in which no liquefaction manifestations were observed, the Darfield earthquake may not have been strong enough to trigger liquefaction and reset the aging clock of the soils, so the age of soil deposits is estimated based on the 1901 Cheviot paleo-EQ scenario. Therefore, in this scenario, a combination of the Darfield EQ and Cheviot paleo-EQ scenarios are considered in determining the aging corrections. As with the Darfield case histories, in which the application of the age-correction resulted in a change in the predicted liquefaction response, the uncorrected predicted liquefaction responses are shown by tails in Figs. 7(c–f).

As shown in Figs. 7(c and d), aging corrections using the Darfield EQ scenario resulted in one additional false-positive (i.e., liquefaction is predicted, but no manifestations were observed) and four additional true-positive (i.e., liquefaction is predicted, and liquefaction manifestations were observed) predictions, resulting in a net decrease of three mispredicted case histories. Similarly, for the combination of the Darfield and Cheviot paleo-EQ scenarios in Figs. 7(e and f), aging corrections resulted in one additional false-positive, and four additional true-positive predictions, resulting in a net decrease of three mispredicted case histories. The additional correct predictions are associated with minor or moderate-to-severe liquefaction case histories moving just above the triggering curve to the liquefaction region. A summary of the error index values and number of mispredicted case histories for the Christchurch database is provided in Fig. 8. As shown in this figure, the number of mispredicted case histories and error index values are the same for both aging correction scenarios. For the combination of the Darfield and Cheviot paleo-EQ scenarios, two of the true-positive liquefaction case histories are moved down and located slightly above the CRR curve close to the no liquefaction region, as illustrated in Figs. 7(e and f). While these two case histories are considered correctly predicted in this study ($FS < 1.0$),

and as a result are not affecting the error index value of this scenario, they are close to the CRR curve and within the level of uncertainty of the simplified liquefaction procedure. This is important to consider especially for the case history with the moderate-severe surficial liquefaction in Fig. 7(f), which would generally be expected to plot further above the CRR curve. As shown in Fig. 8, the error index values are slightly higher for the age-corrected case histories compared to the uncorrected case histories. For the CPT case histories, the error index value increased by the additional false-positive case history that moved over the CRR curve after aging corrections. For the V_s case histories, the error index values increased due to the increase in the CSR values for the four false-positive case histories, moving them further from the CRR line.

Overall, aging corrections improved the liquefaction assessment of the Christchurch case histories. While the error index values are slightly higher for the age-corrected case histories compared to the uncorrected case histories, the number of mispredicted case histories are meaningfully reduced when aging corrections are applied, as shown in Fig. 8. Comparing the number of mispredicted case histories and error index values in Fig. 8, the Darfield EQ scenario resulted in a slightly better performance than the combination of the Darfield EQ and Cheviot paleo-EQ scenarios. This may indicate that the Darfield EQ reset the aging clock for all sites regardless of their surficial liquefaction manifestation, or it may reflect issues with the liquefaction aging procedures for the Christchurch earthquake.

Strong Motion Stations Case Histories during the Christchurch Earthquake

As previously mentioned, the information from both surface manifestations observed by the authors following the Christchurch earthquake and the extensive database of ground motion records for the Christchurch earthquake were used to determine the liquefaction response for each case history. As shown in Table 2, while the observed surficial liquefaction manifestations and characteristics of recorded ground motions are consistent for most of the SMSs case histories, there are three case histories (NNBS1, NNBS2, and REHS) associated with two SMSs (NNBS and REHS) in which no surficial liquefaction manifestations were observed, but clear evidence of liquefaction, including a sharp reduction in the amplitude of ground motion and the loss of high frequency content, was observed in the ground motion records (Wotherspoon et al. 2013). These three case histories are denoted in Fig. 9. As an example, the ground motion records for the PPHS and REHS SMSs

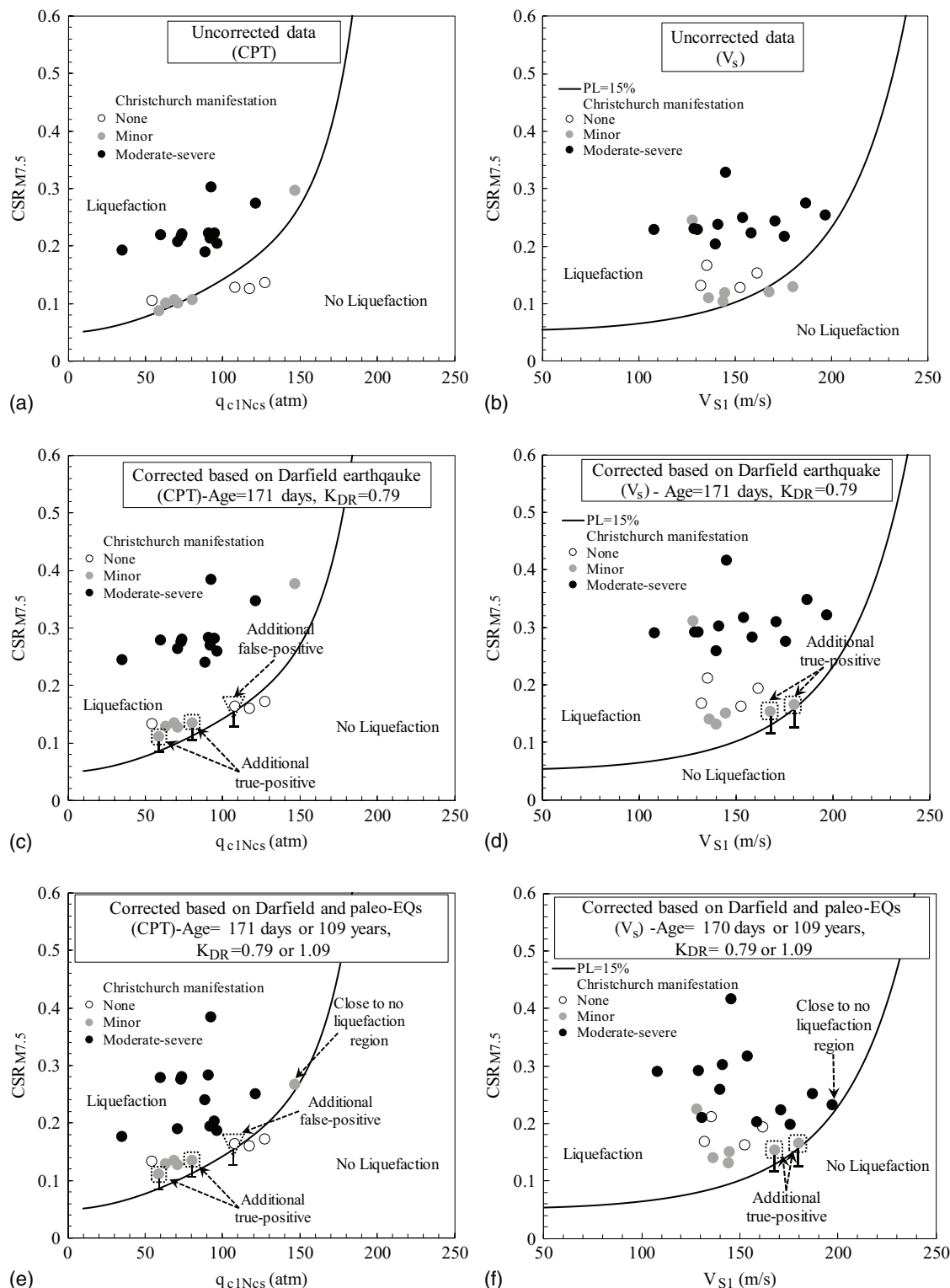


Fig. 7. Uncorrected and age-corrected CPT and V_s liquefaction case histories for the Christchurch earthquake analyzed using the Idriss and Boulanger (2008) and Kayen et al. (2013) triggering procedures: (a) uncorrected data for CPT; (b) uncorrected data for V_s ; (c) age-corrected data for CPT based on the Darfield earthquake; (d) age-corrected data for V_s based on the Darfield earthquake; (e) age-corrected data for CPT based on a combination of the 1901 Cheviot paleo-EQ and Darfield EQ scenarios; and (f) age-corrected data for V_s based on a combination of the 1901 Cheviot paleo-EQ and Darfield EQ scenarios.

during the Christchurch earthquake are shown in Figs. 10(a and b), respectively. A sharp reduction in the amplitude and high-frequency content of the ground motion record at the REHS SMS is observed [Fig. 10(b)], especially in the latter part of this record,

which implies that liquefaction was triggered at this location. However, the record from the PPHS SMS [Fig. 10(a)] does not show any considerable change in the amplitude and frequency content, implying that liquefaction was not triggered at that location.

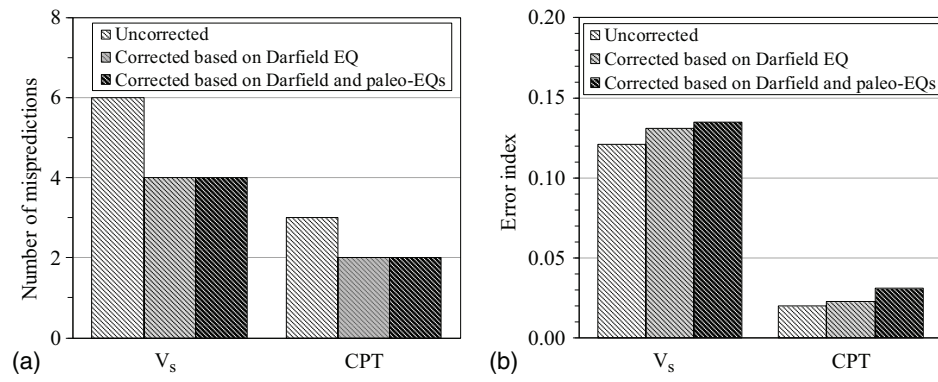


Fig. 8. Evaluation of aging correction efficacy for liquefaction assessment of the Christchurch earthquake using V_s and CPT case histories: (a) number of mispredicted case histories; and (b) error index.

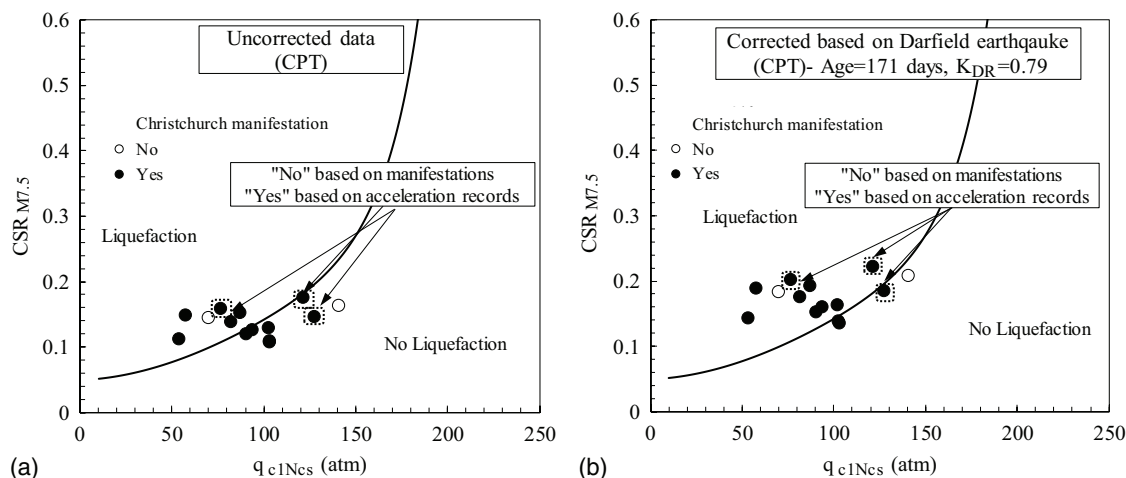


Fig. 9. Uncorrected and age-corrected CPT case histories for the SMSs in Christchurch earthquake analyzed using the Idriss and Boulanger (2008) triggering procedure: (a) uncorrected case histories; and (b) age-corrected case histories.

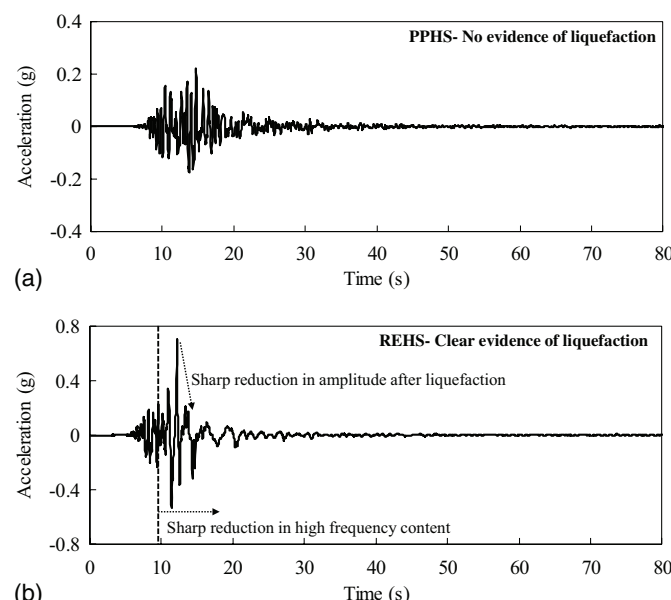


Fig. 10. Ground motion records recorded at the PPHS and REHS SMSs during the Christchurch earthquake: (a) ground motion record at the PPHS SMS showing no evidence of liquefaction; and (b) ground motion record at the REHS SMS showing evidence of liquefaction.

However, no surficial evidence of liquefaction was observed by the authors at the REHS SMS site following the Christchurch event. Therefore, even for cases in which no liquefaction manifestations were observed at the ground surface, it is still possible that the earthquake shaking reset the aging clock of the soil deposits or at least removed a portion of the soil aging effects for earthquakes having magnitudes larger than $\sim Mw 5$ (Green and Bommer 2019), and so this possibility should be considered in liquefaction aging studies.

In Fig. 9, the uncorrected and age-corrected case histories for the SMSs dataset are shown along with tails indicating the initial positions and movements of those case histories in which the aging correction factor moved the case history across the CRR line resulting in a change in their liquefaction prediction. Plotted in Fig. 9(a) are the uncorrected case histories for the CPT measurements, while Fig. 9(b) contains the age-corrected case histories. The Darfield EQ scenario is the only reference point used for the SMSs dataset because this reference point resulted in the lowest error index and number of mispredicted case histories for the previous datasets. As shown in Fig. 9(b), aging corrections moved all the case histories upward, toward the region of predicted liquefaction because the age of soil deposits (171 days) is less than 23 years. Comparing the uncorrected and age-corrected case histories for the SMSs dataset, aging corrections resulted in four additional true-positive liquefaction predictions in the SMSs dataset. Furthermore, there are two

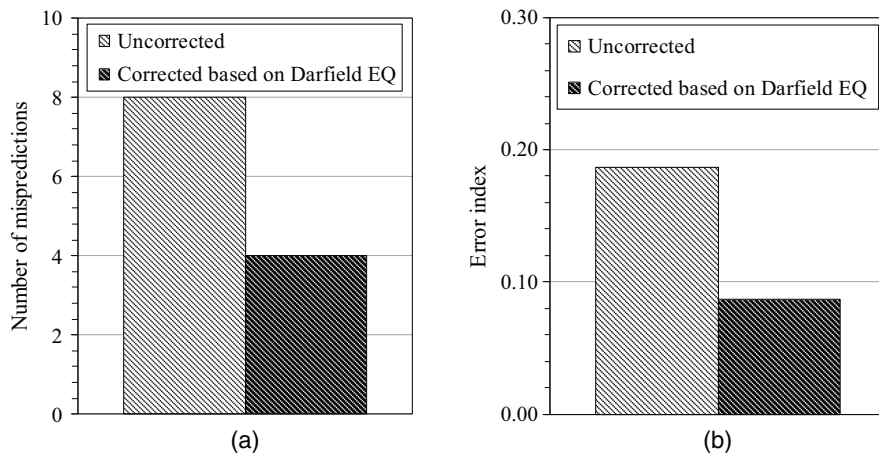


Fig. 11. Evaluation of aging correction efficacy for liquefaction assessment of the SMSs CPT case histories from the Christchurch earthquake: (a) number of mispredicted case histories; and (b) error index.

more false-negative case histories, which are located very close to the region of the predicted liquefaction, as shown in Fig. 9(b). While these points are considered as being mispredicted in this study, they are within the uncertainty range of the simplified liquefaction procedure. The number of mispredicted cases and error index values for the uncorrected and age-corrected case histories are presented in Fig. 11. The error index value for the case histories is significantly reduced from 0.187 to 0.087, and there is a total of four fewer mispredicted case histories.

Overall, aging corrections meaningfully improved the liquefaction assessment of the SMSs case histories by reducing the number of mispredicted case histories and error index values, as shown in Figs. 9 and 11.

Comparison of Aging Correction Efficacy for Darfield, Christchurch, and SMSs Case Histories

Aging corrections were applied to the three liquefaction databases: Darfield, Christchurch, and SMSs. The geological age of the soil deposits in all these databases is Holocene. However, the geotechnical age of the soil deposits was quite different during the Darfield and Christchurch earthquakes. The geotechnical age, defined as the time elapsed since the last critical disturbance, of the soil deposits during the Darfield earthquake is relatively old (i.e., much greater than the reference age), while the soil deposits during the Christchurch earthquake are very young (i.e., much less than the reference age). The results of the aging corrections show that they improved the liquefaction assessment of the Christchurch and SMSs databases (both very young deposits), while their application exacerbated the liquefaction assessment of the Darfield database (relatively old deposits). This exacerbation of the liquefaction assessment of relatively old deposits could be due to the complexities and uncertainties involved in estimating aging effects of relatively old deposits. This issue is also evident in the aging correction factors proposed in the literature because these correction factors were mostly developed based on very young Holocene soil deposits. For example, Hayati and Andrus (2009) developed their aging correction factor using 24 case histories, 14 of which had a geotechnical age less than 20 years and the rest had geotechnical ages ranging between 70 and 35,000,000 years. Therefore, the efficacy of aging correction is questionable for the liquefaction assessment of relatively old soil deposits. However, it should be noted that some of the mispredicted liquefaction case histories from the Darfield

dataset may have been caused by the uncertainty regarding the age estimation of each case history because different case histories may have had different geotechnical ages during the Darfield earthquake (i.e., one of the case history sites may have liquefied in one of the paleo-EQ events, while the others did not liquefy during that same earthquake). Additionally, the five false-positive predictions from the uncorrected Darfield database [shown in Figs. 5(a and b)] may be related to partial saturation issues (e.g., McLaughlin 2017) because the critical layers for some of these case histories are very near to the ground surface, but below the water table, making the liquefaction assessment of these deposits potentially ambiguous. An overestimation of liquefaction potential will result if the soil is assumed to be fully saturated, when in reality, it is only partially saturated, as is sometimes the case for strata within the depth range of water table fluctuation (Ishihara and Tsukamoto 2004; Ishihara et al. 2004). In such cases, false-positive predictions may result. Overall, aging corrections improved the liquefaction assessment of the Christchurch and SMSs databases, which contain very young soil deposits (171 days). These databases consist of many sites that recently liquefied during the Darfield event. For the Christchurch database, the lowest error index value and number of mispredictions were obtained using the Darfield EQ as the reference point for the geotechnical age estimation of all sites regardless of whether or not surficial liquefaction manifestations were observed. This may suggest that the Darfield earthquake likely removed some portion of the soil aging effects for most of the sites with no surficial liquefaction manifestation. If so, the shaking during the event disrupted the soil fabric of the deposits, despite the absence of surficial liquefaction manifestations, thus causing a significant reduction in the CRR of the soil deposits in the next earthquake. Following this same line of reasoning, most of the soils would have behaved like very young soil deposits during the M_w 6.2 Christchurch earthquake.

Examining the age-corrected case histories from the Christchurch and SMSs databases in Figs. 7 and 9, most of the improvements in predictions due to age-corrections are related to case histories that experienced moderate-to-severe liquefaction in the Darfield earthquake and minor liquefaction in the Christchurch earthquake. This trend is also noted by Maurer et al. (2014). All the case histories that experienced moderate-to-severe liquefaction in the Darfield earthquake and minor liquefaction in the Christchurch earthquake are plotted in Fig. 12. These case histories are valuable for assessing the efficacy of the aging corrections because the

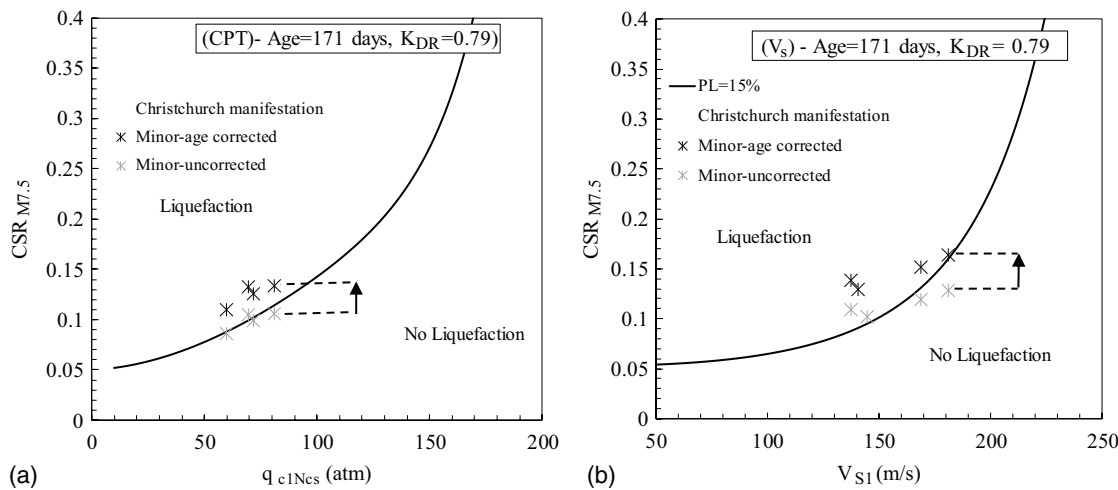


Fig. 12. Uncorrected and age-corrected case histories that experienced moderate-to-severe liquefaction during the Darfield earthquake and minor liquefaction during the Christchurch earthquake: (a) CPT case histories analyzed using the Idriss and Boulanger (2008) triggering procedure; and (b) V_s case histories analyzed using the Kayen et al. (2013) triggering procedure.

moderate-to-severe liquefaction that occurred at these sites during the Darfield earthquake resulted in a complete or near complete loss of aging effects in the soil deposits, and as a result, the geotechnical age of the deposits is relatively well established with a relative uncertainty. During the Christchurch earthquake, these sites only experienced minor liquefaction, and as a result, it would be expected that aging effects will potentially influence the predicted liquefaction response of the sites (i.e., the site is predicted to liquefy versus not liquefy). As shown in Fig. 12, the uncorrected case histories plot close to the CRR triggering curve, with several of the cases being false-negatives. However, when the aging effects are considered, these cases become true-positives, giving credence to the aging correction factors. In contrast, sites that experienced moderate-to-severe liquefaction during the Christchurch earthquake would likely have true-positive predictions, regardless of whether the aging correction factors are applied or not. As a result, their value in assessing the efficacy of the aging correction factors is limited.

Conclusion

Aging corrections were applied to 58 high-quality liquefaction case histories from the M_w 7.1, September 4, 2010, Darfield and the M_w 6.2, February 22, 2011, Christchurch earthquakes to investigate the efficacy of the current liquefaction aging correction procedures. It was determined that the current geological age classification, which is commonly used in geotechnical studies, is insufficient for liquefaction aging investigations. On the other hand, the geotechnical age, which is defined as the time elapsed since the last critical disturbance, seems to be more important for liquefaction aging studies than the geological age. According to the results of the current study, the last critical disturbance and the severity of the liquefaction that occurred during that event are important factors influencing soil aging effects. These factors need to be considered in soil aging studies.

The aging correction factors were determined to exacerbate the liquefaction assessment of relatively old soil deposits, increasing the number of mispredictions and error index. Because the mechanisms underlying soil aging are not well understood and uncertainties involved in the estimation of soil aging effects increase

significantly as deposits age over time, it is difficult to account for aging effects of relatively old soil deposits. Additionally, the lack of reliable case histories for relatively old soil deposits impedes the development of accurate age-correction relationships. On the other hand, correcting for aging considerably improved the liquefaction assessment of sites with very young geotechnical ages, i.e., sites that had experienced shaking from two strong earthquakes in a short period of time in which moderate-to-severe liquefaction was triggered in the first event. For these cases, the occurrence of liquefaction during the first event removed the effect of aging, resulting in a geotechnically young deposit with a well-established geotechnical age.

It is important to consider the possibility that the aging clock of the soil deposit can be reset to zero even for cases in which no surficial liquefaction manifestation was observed (see SMSs case histories). This would be the case for sites in which liquefaction is triggered at depth but does not manifest at the ground surface.

Overall, the cautious use of aging correction is advised for the liquefaction assessment of aged soil deposits due to the inherent complexities of the aging process for relatively old soil deposits (greater than \sim 62–580 years) and the lack of reliable information regarding aging effects of relatively old soil deposits.

Data Availability Statement

Case histories used in this study are available in Green et al. (2014), Wotherspoon et al. (2013), and Wood et al. (2017a, b). Raw CPT and V_s data used in this study are available from the New Zealand Geotechnical database (<https://www.nzgd.org.nz/>) or by request from the corresponding author. Codes used in the study are available from the corresponding author by request.

Acknowledgments

The authors gratefully acknowledge the Canterbury Geotechnical Database and the New Zealand GeoNet project and its sponsors, the Earthquake Commission (EQC), GNS Science, and LINZ, for providing some of the data used in this study. Also, the authors are grateful to Mr. Josh Zupan and Dr. Jonathan Bray, who oversaw the

performance of some of the CPT soundings presented in this study. The primary support for the U.S. authors was provided by the National Science Foundation (NSF) Grant Nos. CMMI-1030564, CMMI-1407428, CMMI-1137977, CMMI-1435494, CMMI-1724575, and CMMI-1825189. Any opinions, findings, conclusions, or recommendations expressed in this material are those of the authors and do not necessarily reflect the views of the NSF or the other funding agencies.

References

Andrus, R. D., H. Hayati, and N. P. Mohanan. 2009. "Correcting liquefaction resistance for aged sands using measured to estimated velocity ratio." *J. Geotech. Geoenvir. Eng.* 135 (6): 735–744. [https://doi.org/10.1061/\(ASCE\)GT.1943-5606.0000025](https://doi.org/10.1061/(ASCE)GT.1943-5606.0000025).

Andrus, R. D., N. P. Mohanan, P. Piratheepan, B. S. Ellis, and T. L. Holzer. 2007. "Predicting shear-wave velocity from cone penetration resistance." In *Proc 4th Int. Conf. on Earthquake Geotechnical Engineering*. Berlin: Springer.

Andrus, R. D., P. Piratheepan, B. S. Ellis, J. Zhang, and C. H. Juang. 2004. "Comparing liquefaction evaluation methods using penetration–Vs relationships." *Soil Dyn. Earthquake Eng.* 24 (9–10): 713–721. <https://doi.org/10.1016/j.soildyn.2004.06.001>.

Andrus, R. D., and K. H. Stokoe II. 2000. "Liquefaction resistance of soils from shear-wave velocity." *J. Geotech. Geoenvir. Eng.* 126 (11): 1015–1025. [https://doi.org/10.1061/\(ASCE\)1090-0241\(2000\)126:11\(1015\)](https://doi.org/10.1061/(ASCE)1090-0241(2000)126:11(1015)).

Arango, I., M. R. Lewis, and C. Kramer. 2000. "Updated liquefaction potential analysis eliminates foundation retrofitting of two critical structures." *Soil Dyn. Earthquake Eng.* 20 (1–4): 17–25. [https://doi.org/10.1016/S0267-7261\(00\)00034-8](https://doi.org/10.1016/S0267-7261(00)00034-8).

Arango, I., and R. E. Miguez. 1996. *Investigation on the seismic liquefaction of old sand deposits*. San Francisco: Bechtel Corporation.

Bastin, S. H., K. Bassett, M. C. Quigley, B. Maurer, R. A. Green, B. Bradley, and D. Jacobson. 2016. "Late Holocene liquefaction at sites of contemporary liquefaction during the 2010–2011 Canterbury earthquake sequence, New Zealand." *Bull. Seismol. Soc. Am.* 106 (3): 881–903. <https://doi.org/10.1785/0120150166>.

Boulanger, R. W., and I. M. Idriss. 2014. *CPT and SPT based liquefaction triggering procedures*. Rep. No. UCD/CGM-14/01. Davis, CA: Center for Geotechnical Modeling, Dept. of Civil and Environmental Engineering, Univ. of California.

Brown, L. J., J. H. Weeber, and J. H. Weeber. 1992. *Geology of the Christchurch Urban Area. Scale 1: 25,000*. Lower Hutt, New Zealand: Institute of Geological & Nuclear Sciences.

Bwambale, B., and R. D. Andrus. 2019. "State of the art in the assessment of aging effects on soil liquefaction." *Soil Dyn. Earthquake Eng.* 125 (Oct): 105658. <https://doi.org/10.1016/j.soildyn.2019.04.032>.

Bwambale, B., R. D. Andrus, and M. Cubrinovski. 2017. "Influence of age on liquefaction resistance of Holocene alluvial and marine soils in Christchurch and Kaiapoi, New Zealand." In *Proc., 3rd Int. Conf. on Performance-based Design in Earthquake Geotechnical Engineering*. London: International Society for Soil Mechanics and Geotechnical Engineering.

Cetin, K. O., and R. B. Seed. 2004. "Nonlinear shear mass participation factor (r_d) for cyclic shear stress ratio evaluation." *Soil Dyn. Earthquake Eng.* 24 (2): 103–113. <https://doi.org/10.1016/j.soildyn.2003.10.008>.

Chuhuan, F. A., A. Kjeldstad, K. Bjorlykke, and K. Hoeg. 2002. "Porosity loss in sand by grain crushing—Experimental evidence and relevance to reservoir quality." *Mar. Pet. Geol.* 19 (1): 39–53. [https://doi.org/10.1016/S0264-8172\(01\)00049-6](https://doi.org/10.1016/S0264-8172(01)00049-6).

Cubrinovski, M., and I. McCahon. 2011. *Foundations on deep alluvial soils*. Christchurch, New Zealand: Univ. of Canterbury.

Green, R. A., and J. J. Bommer. 2019. "What is the smallest earthquake magnitude that needs to be considered in assessing liquefaction hazard?" *Earthquake Spectra*. 35 (3): 1441–1464. <https://doi.org/10.1193/032218EQS064M>.

Green, R. A., M. Cubrinovski, B. Cox, C. Wood, L. Wotherspoon, B. Bradley, and B. Maurer. 2014. "Select liquefaction case histories from the 2010–2011 Canterbury earthquake sequence." *Earthquake Spectra*. 30 (1): 131–153. <https://doi.org/10.1193/030713EQS066M>.

Green, R. A., S. F. Obermeier, and S. M. Olson. 2005. "Engineering geologic and geotechnical analysis of paleoseismic shaking using liquefaction effects: Field examples." *Eng. Geol.* 76 (3–4): 263–293. <https://doi.org/10.1016/j.enggeo.2004.07.026>.

Hayati, H., and R. D. Andrus. 2009. "Updated liquefaction resistance correction factors for aged sands." *J. Geotech. Geoenvir. Eng.* 135 (11): 1683–1692. [https://doi.org/10.1061/\(ASCE\)GT.1943-5606.0000118](https://doi.org/10.1061/(ASCE)GT.1943-5606.0000118).

Hayati, H., R. D. Andrus, S. L. Gassman, M. Hasek, W. M. Camp, and P. Talwani. 2008. "Characterizing the liquefaction resistance of aged soils." In *Geotechnical earthquake engineering and soil dynamics IV*. Reston, VA: ASCE.

Idriss, I. M., and R. W. Boulanger. 2008. *Soil liquefaction during earthquakes*. Berkeley, CA: Earthquake Engineering Research Institute.

Ishihara, K. 1996. *Soil behavior in earthquake geotechnics*. New York: Oxford University Press.

Ishihara, K., and Y. Tsukamoto. 2004. "Cyclic strength of imperfectly saturated sands and analysis of liquefaction." *Proc. Japan Acad., Series B* 80 (8): 372–391. <https://doi.org/10.2183/pjab.80.372>.

Ishihara, K., Y. Tsukamoto, and K. Kamada. 2004. "Undrained behavior of near-saturated sand in cyclic and monotonic loading." In *Proc. Conf. Cyclic Behavior of Soils and Liquefaction Phenomena*, 27–39. Abingdon, UK: Taylor & Francis.

Joshi, R. C., G. Achari, S. R. Kaniraj, and H. Wijeweera. 1995. "Effect of aging on the penetration resistance of sands." *Can. Geotech. J.* 32 (5): 767–782. <https://doi.org/10.1139/t95-075>.

Kayen, R., R. E. S. Moss, E. M. Thompson, R. B. Seed, K. O. Cetin, A. D. Kiureghian, A. Der Kiureghian, Y. Tanaka, and K. Tokimatsu. 2013. "Shear-wave velocity-based probabilistic and deterministic assessment of seismic soil liquefaction potential." *J. Geotech. Geoenvir. Eng.* 139 (3): 407–419. [https://doi.org/10.1061/\(ASCE\)GT.1943-5606.0000743](https://doi.org/10.1061/(ASCE)GT.1943-5606.0000743).

Kiyota, T., J. Koseki, T. Sato, and R. Kuwano. 2009. "Aging effects on small strain shear moduli and liquefaction properties of in-situ frozen and reconstituted sandy soils." *Soils Found.* 49 (2): 259–274. <https://doi.org/10.3208/sandf.49.259>.

Kulhawy, F. H., and P. W. Mayne. 1990. *Manual on estimating soil properties for foundation design*. Rep. No. EPRI-EL-6800. Ithaca, NY: Cornell Univ.

Leon, E., S. L. Gassman, and P. Talwani. 2006. "Accounting for soil aging when assessing liquefaction potential." *J. Geotech. Geoenvir. Eng.* 132 (3): 363–377. [https://doi.org/10.1061/\(ASCE\)1090-0241\(2006\)132:3\(363\)](https://doi.org/10.1061/(ASCE)1090-0241(2006)132:3(363)).

Lewis, M. R., M. D. McHood, and I. Arango. 2004. "Liquefaction evaluations at the Savannah river site. A case history." In *Proc., 5th Int. Conf. on Case Histories in Geotechnical Engineering*. Rolla, MO: Univ. of Missouri.

Maurer, B. W., R. A. Green, M. Cubrinovski, and B. A. Bradley. 2014. "Assessment of aging correction factors for liquefaction resistance at sites of recurrent liquefaction." In *Proc., 10th National Conf. on Earthquake Engineering (10NCEE)*. Oakland, CA: Earthquake Engineering Research Institute.

McLaughlin, K. A. 2017. "Investigation of false-positive liquefaction case history sites in Christchurch, New Zealand." M.S. thesis, Dept. of Civil, Architectural, and Environmental Engineering, Univ. of Texas at Austin.

Mesri, G., T. W. Feng, and J. M. Benak. 1990. "Postdensification penetration resistance of clean sands." *J. Geotech. Eng.* 116 (7): 1095–1115. [https://doi.org/10.1061/\(ASCE\)0733-9410\(1990\)116:7\(1095\)](https://doi.org/10.1061/(ASCE)0733-9410(1990)116:7(1095)).

Mitchell, J. K. 1986. "Practical problems from surprising soil behavior." *J. Geotech. Eng.* 112 (3): 255–289. [https://doi.org/10.1061/\(ASCE\)0733-9410\(1988\)114:3\(367\)](https://doi.org/10.1061/(ASCE)0733-9410(1988)114:3(367)).

Mitchell, J. K., and Z. V. Solymar. 1984. "Time-dependent strength gain in freshly deposited or densified sand." *J. Geotech. Eng.* 110 (11): 1559–1576. [https://doi.org/10.1061/\(ASCE\)0733-9410\(1984\)110:11\(1559\)](https://doi.org/10.1061/(ASCE)0733-9410(1984)110:11(1559)).

Moss, R. E., R. B. Seed, R. E. Kayen, J. P. Stewart, A. Der Kiureghian, and K. O. Cetin. 2006. "CPT-based probabilistic and deterministic assessment of in situ seismic soil liquefaction potential." *J. Geotech. Geoenvir. Eng.* 132 (5): 407–419. [https://doi.org/10.1061/\(ASCE\)GT.1943-5606.0000743](https://doi.org/10.1061/(ASCE)GT.1943-5606.0000743).

Geoenviron. Eng. 132 (8): 1032–1051. [https://doi.org/10.1061/\(ASCE\)1090-0241\(2006\)132:8\(1032\)](https://doi.org/10.1061/(ASCE)1090-0241(2006)132:8(1032)).

Olson, S. M., R. A. Green, and S. F. Obermeier. 2005. “Geotechnical analysis of paleoseismic shaking using liquefaction features: A major updating.” *Eng. Geol.* 76 (3–4): 235–261. <https://doi.org/10.1016/j.enggeo.2004.07.008>.

Olson, S. M., S. F. Obermeier, and T. D. Stark. 2001. “Interpretation of penetration resistance for back-analysis at sites of previous liquefaction.” *Seismol. Res. Lett.* 72 (1): 46–59. <https://doi.org/10.1785/gssrl.72.1.46>.

Rahimi, S., C. M. Wood, F. Coker, T. Moody, M. Bernhardt-Barry, and B. M. Kouchaki. 2018. “The combined use of MASW and resistivity surveys for levee assessment: A case study of the Melvin Price Reach of the Wood River Levee.” *Eng. Geol.* 241 (Jul): 11–24. <https://doi.org/10.1016/j.enggeo.2018.05.009>.

Roy, D., R. G. Campanella, P. M. Byrne, and J. M. O. Hughes. 1996. “Strain level and uncertainty of liquefaction related index tests.” In *Uncertainty in the geologic environment: From theory to practice*, 1149–1162. New York: ASCE.

Saftner, D. A., R. A. Green, and R. D. Hryciw. 2015. “Use of explosives to investigate liquefaction resistance of aged sand deposits.” *Eng. Geol.* 199 (Dec): 140–147. <https://doi.org/10.1016/j.enggeo.2015.11.002>.

Schmertmann, J. H. 1987. “Discussion of ‘Time-dependent strength gain in freshly deposited or densified sand’ by James K. Mitchell and Zoltan V. Solymar (November, 1984).” *J. Geotech. Eng.* 113 (2): 173–175. [https://doi.org/10.1061/\(ASCE\)0733-9410\(1987\)113:2\(173\)](https://doi.org/10.1061/(ASCE)0733-9410(1987)113:2(173)).

Seed, H. B., and I. M. Idriss. 1971. “Simplified procedure for evaluating soil liquefaction potential.” *J. Soil Mech. Found. Div.* 97 (9): 1249–1273.

Towhata, I., S. Maruyama, K. I. Kasuda, J. Koseki, K. Wakamatsu, H. Kiku, T. Kiyota, S. Yasuda, Y. Taguchi, A. Aoyama, and T. Hayashida. 2014. “Liquefaction in the Kanto region during the 2011 off the pacific coast of Tohoku earthquake.” *Soils Found.* 54 (4): 859–873. <https://doi.org/10.1016/j.sandf.2014.06.016>.

Towhata, I., Y. Taguchi, T. Hayashida, S. Goto, Y. Shintaku, Y. Hamada, and S. Aoyama. 2017. “Liquefaction perspective of soil ageing.” *Géotechnique* 67 (6): 467–478. <https://doi.org/10.1680/jgeot.15.P.046>.

Upadhyaya, S., R. A. Green, A. Rodriguez-Marek, B. W. Maurer, L. Wotherspoon, B. A. Bradley, and M. Cubrinovski. 2019. “Influence of corrections to recorded peak ground accelerations due to liquefaction on predicted liquefaction response during the 2010–2011 Canterbury, New Zealand, earthquake sequence.” In *Proc. 13th Australia New Zealand Conf. on Geomechanics*. Perth, Australia.

Whitman, R. V. 1971. “Resistance of soil to liquefaction and settlement.” *Soils Found.* 11 (4): 59–68. https://doi.org/10.3208/sandf1960.11.4_59.

Wood, C. M., B. R. Cox, R. A. Green, L. M. Wotherspoon, B. A. Bradley, and M. Cubrinovski. 2017a. “Vs-based evaluation of select liquefaction case histories from the 2010–2011 Canterbury earthquake sequence.” *J. Geotech. Geoenviron. Eng.* 143 (9): 04017066. [https://doi.org/10.1061/\(ASCE\)GT.1943-5606.0001754](https://doi.org/10.1061/(ASCE)GT.1943-5606.0001754).

Wood, C. M., C. R. McGann, B. R. Cox, R. A. Green, L. M. Wotherspoon, and B. A. Bradley. 2017b. “A comparison of CPT-Vs correlations using a liquefaction case history database from the 2010–2011 Canterbury earthquake sequence.” In *Proc., 3rd Int. Conf. on Performance-based Design in Earthquake Geotechnical Engineering (PBD-III)*. London: International Society for Soil Mechanics and Geotechnical Engineering.

Wotherspoon, L. M., R. Orense, B. A. Bradley, B. R. Cox, C. Wood, and R. A. Green. 2013. “Geotechnical characterization of Christchurch strong motion stations.” In *Version 1.0, Earthquake Commission Report*. Auckland, New Zealand: Univ. of Auckland.

Youd, T. L., et al. 2001. “Liquefaction resistance of soils: Summary report from the 1996 NCEER and 1998 NCEER/NSF workshops on evaluation of liquefaction resistance of soils.” *J. Geotech. Geoenviron. Eng.* 127 (10): 817–833. [https://doi.org/10.1061/\(ASCE\)1090-0241\(2001\)127:10\(817\)](https://doi.org/10.1061/(ASCE)1090-0241(2001)127:10(817)).

Youd, T. L., and S. N. Hoose. 1977. “Liquefaction susceptibility and geologic setting.” In Vol. 6 of *Proc. 6th World Conf. on Earthquake Engineering*, 37–42. Roorkee, India: Indian Society of Earthquake Technology.

Youd, T. L., and D. M. Perkins. 1978. “Mapping liquefaction-induced ground failure potential.” *J. Soil Mech. Found. Div.* 104 (4): 433–446.